Zhou, Man; Cao, Zhixian; Yue, Zhiyuan; Li, Kanyu

Full Hydrodynamic Modeling of Flash Flooding Due to Heavy Rainfall

FULL HYDRODYNAMIC MODELING OF FLASH FLOODING DUE TO HEAVY RAINFALL

Man Zhou[1], Zhixian Cao[2], Zhiyuan Yue[1], and Kanyu Li[1]

[1] Research assistant, State Key Laboratory of Water Resources and Hydropower Engineering Science, Wuhan University, Wuhan 430072, China.

[2] Corresponding author, Professor, State Key Laboratory of Water Resources and Hydropower Engineering Science, Wuhan University, Wuhan 430072, China. E-mail: zxcao@whu.edu.cn

ABSTRACT

A two-dimensional full hydrodynamic model is developed for modeling flash flooding generated by temporally and spatially variable rainfall. The governing equations of the model comprise the complete shallow water hydrodynamic equations closed with Manning roughness for boundary resistance and Green-Ampt formulation for infiltration loss. The second-order Total-Variation-Diminishing version of the Weighted-Average-Flux method, along with the HLL approximate Riemann Solver, is used to solve the governing equations, which can properly resolve shock waves. A series of numerical tests with regular bottom surfaces demonstrate the ability of the full hydrodynamic model to effectively reproduce runoff hydrographs downstream and the specific flow structure, such as roll waves that are prone to occur over steep slopes. In contrast, without incorporating the full mechanisms of overland and mountain river flows, traditional models based on kinematic and diffusion wave approximations are unable to properly resolve roll waves. The proposed model is applied to a complex terrain condition with presumed rainfall scenarios. The need for boundary conditions is actually obviated by extending the computational domain over the region of interest so that the flow has not arrived at the boundaries of the domain during the time period of computation. Temporal variation and spatial distribution of rainfall and infiltration are shown to be effective in dictating the magnitude of the peak discharge, the hydrograph shape and the time to peak. Nonlinear relationship between rainfall and runoff is found for a watershed with irregular topography, which seems to upset previous models based on the concept of unit-hydrographs or its variants, and also necessitates the full hydrodynamic modeling paradigm.

Keywords: flash flooding, shallow water hydrodynamics, infiltration, boundary condition, rainfall-runoff relationship

1. INTRODUCTION

The last several decades have seen great improvements in flash flood prediction, with progresses in the development of physically based mathematical models, including simplified models and more general models based on St-Venant equations. Yet without incorporating the full mechanisms of overland and mountain river flows, kinematic and diffusion wave models are unable to properly represent flash flood generation and propagation, such as roll waves that are prone to occur over steep channels (Liu *et al.,* 2004; Jain *et al.,* 2004). One-dimensional (1D) hydrodynamic models based on full St-Venant equations feature the major mechanisms of flow,

and thus are potentially able to simulate flash flood, but may fail for flash flood propagation over irregular slopes (Cao and Yue, 2007). Given this observation, two-dimensional (2D) full hydrodynamic modeling methodology is necessary for enhanced flash flood prediction (Esteves *et al.,* 2000; Fiedler and Ramirez, 2000).

This paper presents a 2D full hydrodynamic model to simulate rainfall-triggered flash flooding, of which the governing equations are numerically solved using the second-order Total-Variation-Diminishing (TVD) version of the Weighted-Average-Flux (WAF) method along with the HLL approximate Riemann Solver. A series of numerical tests are carried out to demonstrate the ability of the present model to route overland flow downstream and resolve roll waves. The present model is applied to a complex terrain condition with variable rainfall and infiltration, which are shown to be sensitive parameters on runoff hydrographs. Rainfall-runoff relationship is analyzed and nonlinear response is found over irregular topography.

2. SHALLOW WATER HYDRODYNAMIC MODELS

2.1 Governing equations

The governing equations of shallow water hydrodynamic models can be derived from the basic conservation laws in fluid dynamics (Cunge *et al.*, 1980). As rainfall and infiltration loss are incorporated, one has

$$\frac{\partial \mathbf{U}}{\partial t} + \frac{\partial \mathbf{F}}{\partial x} + \frac{\partial \mathbf{G}}{\partial y} = \mathbf{S} \tag{1}$$

$$\mathbf{U} = \begin{bmatrix} h \\ hu \\ hv \end{bmatrix},\ \mathbf{F} = \begin{bmatrix} hu \\ hu^2 + gh^2/2 \\ huv \end{bmatrix},\ \mathbf{G} = \begin{bmatrix} hv \\ huv \\ hv^2 + gh^2/2 \end{bmatrix},\ \mathbf{S} = \begin{bmatrix} r - f \\ gh(S_{bx} - S_{fx}) \\ gh(S_{by} - S_{fy}) \end{bmatrix} \tag{2a,b,c,d}$$

where $\mathbf{U}$ = vector of conserved variables; $\mathbf{F}, \mathbf{G}$ = vectors of flux variables; $\mathbf{S}$ = vector of source terms; t = time; x, y = horizontal coordinates; h = flow depth; u, v = depth-averaged velocities in the x - and y -directions; r = rainfall intensity; f = infiltration rate; g = gravitational acceleration; S_{fx}, S_{fy} = friction slope in x - and y -directions; S_{bx}, S_{by} = bed slope in x - and y -directions, $S_{bx} = -\partial z / \partial x$, $S_{by} = -\partial z / \partial y$ respectively, and z = bed elevation.

2.2 Empirical closure relationship

The friction slopes are determined using the conventional relationship, which involves the Manning roughness n

$$S_{fx} = \frac{n^2 u\sqrt{u^2 + v^2}}{h^{4/3}}, \qquad S_{fy} = \frac{n^2 v\sqrt{u^2 + v^2}}{h^{4/3}} \tag{3}$$

The infiltration rate f is defined by the Green-Ampt equation

$$f = \frac{dF}{dt} = K_s(1 + \frac{(\theta_s - \theta_i)H_c}{F}) \tag{4a}$$

$$F = K_s t + H_c(\theta_s - \theta_i)\ln(1 + \frac{F}{(\theta_s - \theta_i)H_c}) \tag{4b}$$

where K_s = saturated hydraulic conductivity; H_c = Green-Ampt capillary head term; θ_s, θ_i = the saturated and initial volumetric water content; F = cumulative infiltrated depth. The pattern of infiltration excess runoff is adopted as for arid and semi-arid environments in contrast to that of saturated excess runoff for humid areas. At the onset of a rainfall event, when rainfall intensity is lower than the infiltration capacity, all the rainfall infiltrates, the actual infiltration rate is equal to the rainfall rate and there is no runoff on the surface. As rainfall continues, the infiltration capacity decreases. When this capacity equals or less than the rainfall rate, water will pond on the soil surface. After ponding has taken place, the actual infiltration rate is equal to the infiltration capacity (Esteves *et al*., 2000).

2.3 Numerical scheme

The second-order WAF-TVD algorithm along with the HLL approximate Riemann solver is used to numerically solve the governing equations, which can properly capture shock waves. This is essentially a slightly adapted version of the more general numerical algorithm shallow water flow, sediment transport and morphological evolution, as reported in Cao *et al.* (2007).

3. NUMERICAL TESTS

Woolhiser *et al.* (1996) examine the effects of spatial variability of saturated hydraulic conductivity K_s on surface runoff utilizing a 1D kinematic wave model with Smith-Parlange equation. Fiedler and Ramirez (2000) investigate the interaction between infiltration and surface water component using the full hydrodynamic flow equations incorporating the Green-Ampt equation. The same numerical tests specified by Woolhiser *et al.* (1996) and Fiedler and Ramirez (2000) are deployed in this section to test the present hydrodynamic model. A comparison is presented between the present 2D hydrodynamic model and a 1D kinematic wave model closed with Green-Ampt equation. The 1D kinematic wave model is numerically solved using the conventional method of characteristics, and the spatial step Δx and time step Δt are equal to 0.25 m and 0.1 s respectively. For the 2D hydrodynamic model, the spatial step Δx = 0.25 m is used and the time step is specified according to the stability condition defined by the Courant number Cr = 0.04 to insure that the time step is approximately consistent with the 1D kinematic wave model. The computational reach is set to be 50 m, and other parameters are given in Table 1. Figure 1 shows the discharge hydrographs from the kinematic wave model and the present hydrodynamic model (Cases 1, 2 and 3, Table 1). Satisfactory agreement between the two models is evident for the particular case.

Table 1. Summary of Parameters

Case No.	Soil Parameters			Hillslope Parameters		Rainfall	
	K_s (cm/min)	$\theta_s - \theta_i$	H_c (cm)	S_b	n	Rate r (cm/min)	Duration t (min)
1	0.0212	0.25	44	0.04	0.1	0.296	20
2	$0.0212(1.3303\text{-}0.6606\,x/L)$	0.25	44	0.04	0.1	0.296	20
3	$0.0212(0.6697\text{+}0.6606\,x/L)$	0.25	44	0.04	0.1	0.296	20

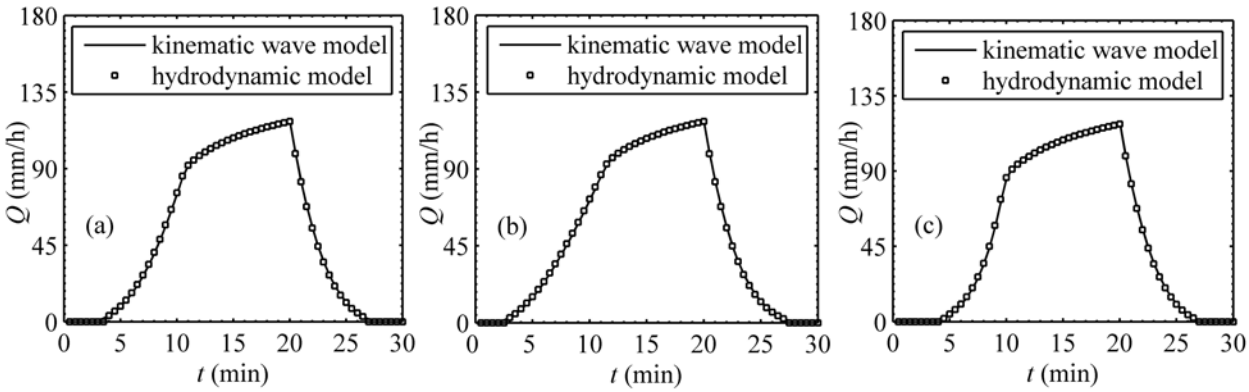

Figure 1. Discharge hydrographs for (a) Case 1, (b) Case 2, and (c) Case 3

If the channel is sufficiently steep and long, a series of waves, usually referred to as roll waves, can be observed, which have been investigated in many prior studies (e.g., Brock, 1969; Zanuttigh and Lamberti, 2002; Liu *et al.,* 2005). The purpose herein is to test the ability of the present 2D hydrodynamic model to reproduce roll waves, as compared to the 1D hydrodynamic model (Li *et al*., 2008). The numerical test is conducted for a channel of length 400 m. The bed slope S_b = 0.05 and Manning roughness n = 0.01. The initial water depth and unit-width discharge for the upstream are h_0 = 0.008 m, q_0 = 0.007155 m^2/s, Froude number Fr = 3.194. At the inlet, a periodic disturbance is imposed as $h' = h_0(1 + 0.005\sin(\pi t))$. The simulations are performed using Δx = 0.05 m and Cr = 0.5.

Figure 2a shows the flow depth profiles at t =250 s by 1D and 2D models, and Figure 2b the free surface profiles. Typical transient flow depths at x = 13 m and x =70 m are illustrated in Figures 2c and 2d. It is seen that both the 1D and 2D hydrodynamic models effectively reproduce roll waves. Yet the roll waves resolved by the 2D model appear to have evolved to a fully developed state appreciably sooner than from the 1D model. This may be attributed to the additional transverse numerical disturbances in the 2D model.

The kinematic wave approximation presumes that the friction slope (S_f in one dimension) is equal to bed slope, i.e., $S_f = S_b$; and the diffusion wave approximation assumes that $\partial h/\partial x + S_f = S_b$. However, as resolved by the present hydrodynamic 2D model, the values of

S_f and $\partial h/\partial x + S_f$ deviate significantly from that of S_b, as illustrated in Figure 3. It follows that the kinematic and diffusion wave approximations are not applicable for overland flows featuring roll waves.

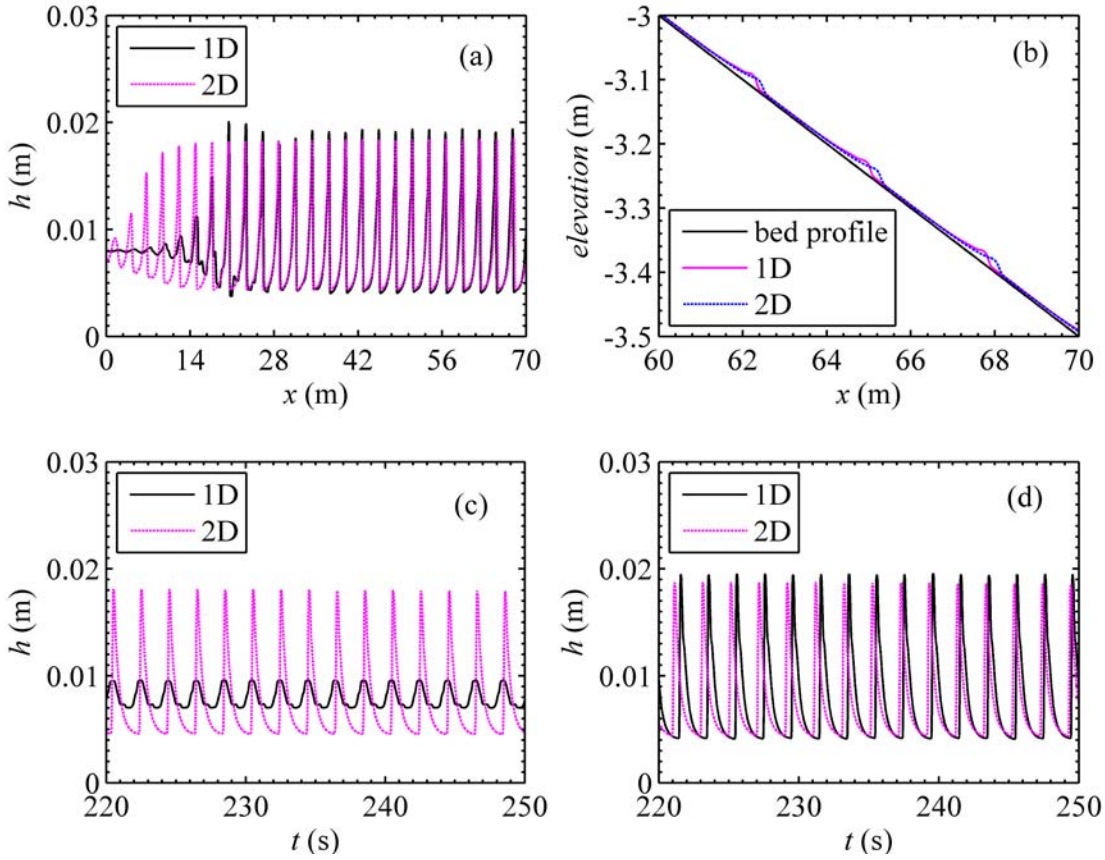

Figure 2. Flow depth (a) and free surface (b) profiles at t=250 s; transient flow depth at x= 13 m (c) and x=70 m (d)

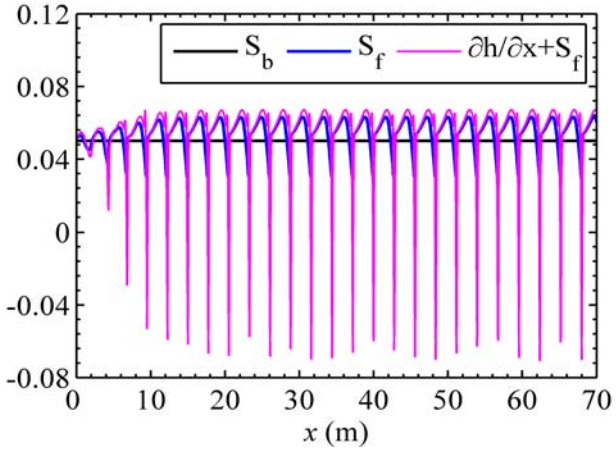

Figure 3. Profiles of S_b, S_f and $\partial h/\partial x + S_f$ from the present hydrodynamic model

4. PRELIMINARY APPLICATIONS

4.1 Hydrographs

Surface runoff sensitivity to spatial and temporal variability of rainfall has been examined using distributed hydrological models (e.g., Hjelmfelt, 1981; Ogden and Julien, 1993). Here the effects of rainfall and infiltration over complex topography are addressed by applying the present 2D hydrodynamic model to Tianshui region in Gansu Province in China, which covers an area of about 723.35 km^2 (0 km$\le x \le$ 29.05 km, 0 km$\le y \le$ 24.9 km), the computational domain. To obviate the need for boundary conditions, an area of 289.33 km^2 is specified as rainfall area (4.98 km$\le x \le$ 22.41 km, 4.15 km$\le y \le$ 20.75 km) so that the flow has not arrived at the boundaries of the computational domain during the whole time period of computation (4 hrs). The spatial step is 83 m both in x- and y-directions, the time step is specified by Cr = 0.015, and Manning roughness n = 0.04. The rainfall and infiltration are varied in the numerical test cases, as summarized in Table 2. The total volume of rainfall is the same in the four cases. The first three cases neglect the infiltration loss, whilst it is considered in Case 4.

Table 2. Values of rainfall rate and infiltration for four cases

Case No.	Rainfall intensity (mm/h)	Distribution (h)	Infiltration
1	200	$0 \le t \le 1.0$	Without infiltration
	0	$1.0 < t \le 4.0$	
2	267	$0 \le t \le 0.25$	
	133	$0.25 < t \le 0.5$	
	267	$0.5 < t \le 0.75$	
	133	$0.75 < t \le 1.0$	
	0	$1.0 < t \le 4.0$	
3	100	$0 \le t \le 2.0$	
	0	$2.0 < t \le 4.0$	
4	267	$0 \le t \le 0.25$	$K_s = 1.67 \times 10^{-6}$ m/s $\theta_s = 0.5$ $\theta_i = 0.25$ $H_c = 0.5$ m
	133	$0.25 < t \le 0.5$	
	267	$0.5 < t \le 0.75$	
	133	$0.75 < t \le 1.0$	
	0	$1.0 < t \le 4.0$	

Figure 4 shows the propagation of the flash flood for Case 2, as represented by water surface level. It is seen that the flood flows into low-lying areas and appears to follow concentrated flow routes under the gravitational action. As the computational time increases, the flood flow extends beyond the rainfall area, and one of the wave fronts has nearly arrived at the downstream boundary of the computational domain (x = 29 km).

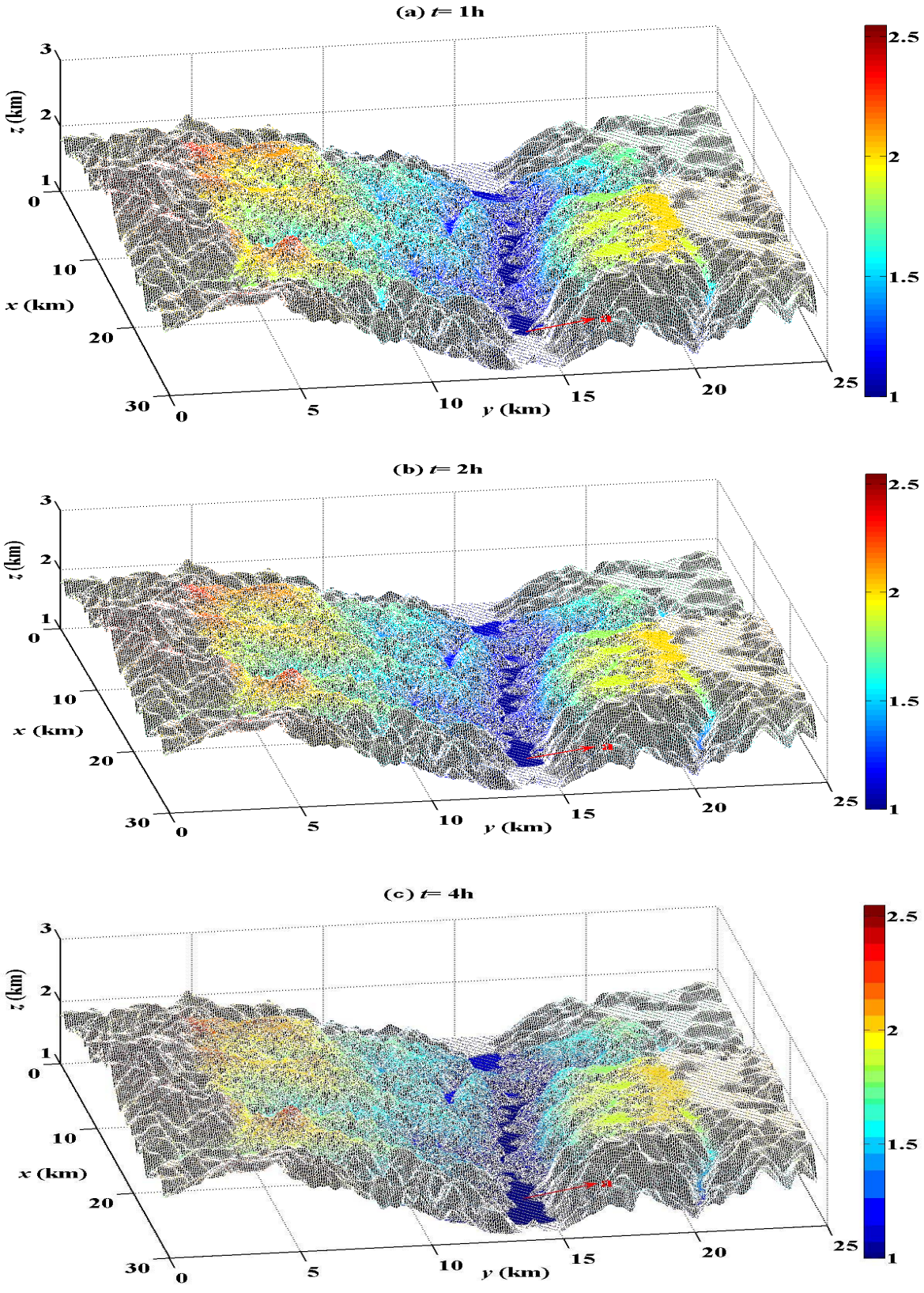

Figure 4. Propagation of flash flood: evolution of water surface level

For analysis of the computed hydrographs, a near-outlet cross-section is specified at x = 22.41 km, and a particular point a designated (x = 22.41 km, y = 14.27 km). Figures 5a and 5b illustrate respectively the discharge hydrographs at the specified cross-section and stage hydrographs at point a. Cases 1 and 2 assume the same duration and total volume of rainfall but distinct rainfall intensity, the resulting hydrographs appear not to be so sensitive to the temporal variation of rainfall intensity. However, as the same total volume of rainfall is distributed over a longer duration with lower intensity (Cases 1 and 3, Table 2), the discharge and stage hydrographs are greatly altered. Specifically, the peak discharge and stage are reduced, and the time to peak is considerably delayed. Further, the infiltration loss can remarkably affect the hydrographs (Cases 2 and 4, Table 2). When infiltration is considered, the peak discharge and stage are largely decreased, and an appreciable delay of the occurrence of peaks is found. Also of interest is the observation that the peak discharge and stage may come considerably after the rainfall ceases, which represents a time lag effect between the maximum accumulated rainfall and the time to peak hydrographs. In conclusion, rainfall intensity and infiltration are among the key factors affecting flash flood hydrographs.

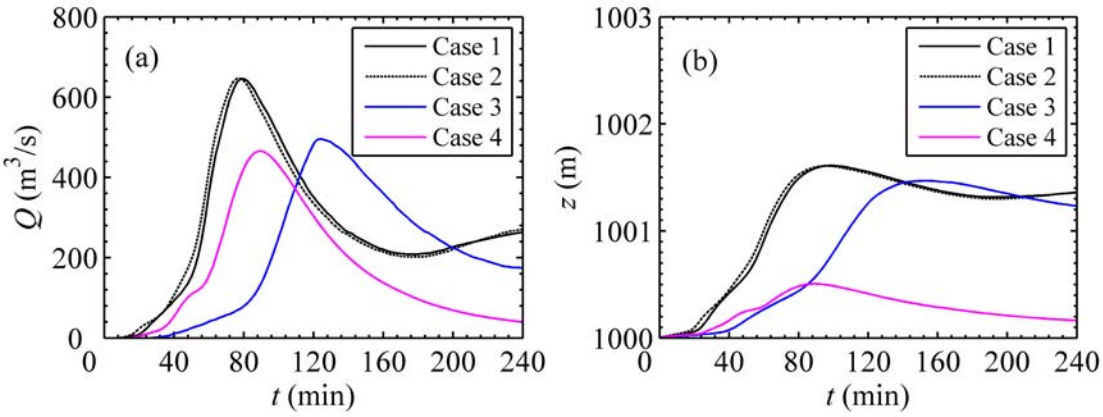

Figure 5. (a) Discharge hydrographs at the specified near-outlet cross-section, and (b) stage hydrographs at point a

4.2 Rainfall-runoff relationship

There have been a number of linear models proposed to describe the rainfall-runoff transformation. Those based on the concept of unit hydrograph (UH) are probably the most widely used, which however are limited by the potential nonlinearity as related to the soil, vegetation, topography characteristics and also the distribution, duration and intensity of rainfall in natural watersheds (Jain *et al.,* 2004; Saghafian, 2006). Julien *et al*. (1995) effectively resolve the nonlinear response of watershed, yet their work is based on diffusion wave approximation CASC2D. This section aims to address the rainfall-runoff relationship using the present 2D full hydrodynamic model. In this analysis, the rainfall-runoff relationship is examined for two distinct topography situations (regular and complex). A regular topography with a mean slope of 0.015 is selected (Iwagaki, 1955), and a complex topography for Tianshui watershed is used.

Figure 6 shows the relationship between rainfall (P) and runoff (R) over regular and complex topography scenarios with distinct rainfall intensity. Linear relationship between rainfall and runoff apparently exists over regular topography independent of rainfall conditions (Figure 6a). This appears to support the applicability of traditional linear models, such as the UH-based techniques. In contrast, nonlinear relationship is found over complex topography as shown in Figure 6b. This follows that complex topography is a crucial factor that leads to nonlinear relationship between rainfall and runoff. Therefore flash flood prediction methodologies based on linear principles may not be appropriate for natural complex topography, and full hydrodynamic model is essential, which does not evoke the linearity constraint between rainfall and runoff.

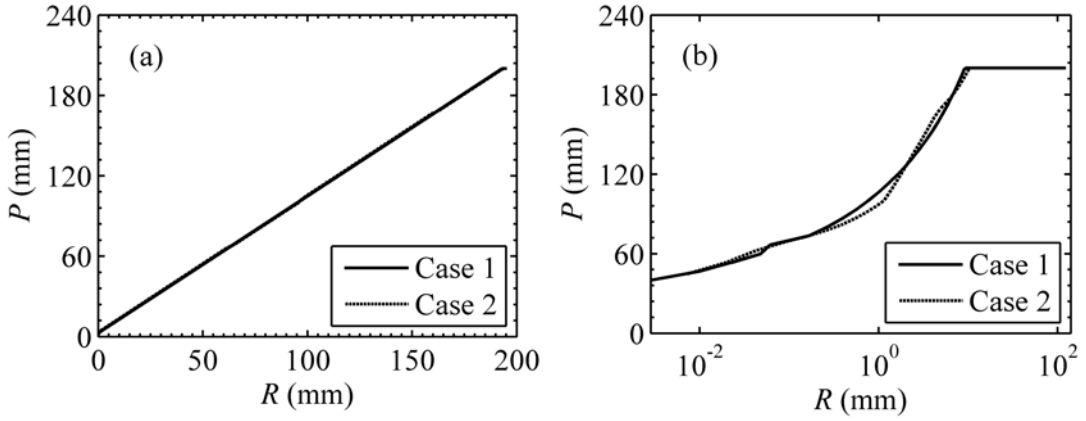

Figure 6. Rainfall-runoff relationship over (a) regular topography, and (b) complex topography

5. CONCLUSION

A 2D full hydrodynamic model capable of simulating rainfall-induced flash flooding is proposed. The model is based on the complete shallow water hydrodynamic equations, incorporating boundary resistance and infiltration loss. The governing equations are numerically solved with a second-order WAF-TVD algorithm along with the HLL approximate Riemann Solver. A series of numerical tests demonstrate the ability of the model to simulate runoff hydrographs downstream and the specific flow structure, such as roll waves, which however cannot be properly resolved by traditional distributed hydrological models based on kinematic and diffusion wave approximations. The proposed model is applied to a complex topography with variable rainfall and infiltration, which have been shown to be sensitive parameters on runoff predictions. Nonlinear relationship is found between rainfall and runoff over irregular topography, which illustrates that traditional UH-based runoff approaches are ineffective, and also necessitates the full hydrodynamic modeling paradigm.

ACKNOWLEDGMENTS

The work reported in this manuscript is part of the research program funded by Natural Science Foundation of China (Grant No. 50739002) and the EU 6th Framework Program under Project HYDRATE (Grant No. 037024).

REFERENCES

Brock, R.R. (1969), Development of roll wave trains in open channels, *Journal of Hydraulics Division*, 95(4), pp.1401-1425.

Cao, Z.X. and Yue, Z.Y. (2007), Comment on "Investigation of the hydrodynamics of flash floods in ephemeral channels: scaling analysis and simulation using a shock-capturing flow model incorporating the effects of transmission losses" by S M Mudd, 2006, Journal of Hydrology 324, 65-79, *Journal of Hydrology*, 336, pp.222-225.

Cao, Z.X., Yue, Z.Y., Li, X., Che, T. (2007), Two-dimensional mathematical modeling of flooding over erodible sediment bed, *Proc. 32nd IAHR Congress*, July 1-6, Venice, Italy.

Cunge, J.A., Holly, F.M., Verwey, A. (1980), Practical aspects of computational river hydraulics, *London, Pitman Pub*.

Esteves, M., Faucher, X., Galle, S., Vauclin, M. (2000), Overland flow and infiltration modeling for small plots during unsteady rain: numerical results versus observed values, *Journal of Hydrology*, 228, pp.265-282.

Fiedler, F.R. and Ramirez, J.A. (2000), A numerical method for simulating discontinuous shallow flow over an infiltrating surface, *International Journal of Numerical Methods in Fluids,* 32(2), pp.219-240.

Hjelmfelt, A.T. (1981), Overland flow from time-distributed rainfall, J*ournal of Hydraulics Division*, 107(2), pp.227-238.

Iwagaki, Y. (1955), Fundamental studies on the runoff analysis by characteristics, *Disaster Prevention Research Institute Bulletin*, 10, Kyoto University, Kyoto, Japan.

Jain, M.K., Kothyari, U.C., Raju, K.G. (2004), A GIS based distributed rainfall-runoff model, *Journal of Hydrology*, 299, pp.107-135.

Julien, P.Y., Saghafian, B., Ogden, F.L. (1995), Raster-based hydrologic modeling of spatially-varied surface runoff, *Water Resources Bulletin*, 31(3), pp.523-536.

Li, K., Cao, Z.X., Liu, Q.Q. (2008), Computational study of roll waves in shallow flow over erodible bed, *8th International Conference on Hydroscience & Hydraulic Engineering*, September 8-12, Nagoya, Japan.

Liu, Q.Q., Chen, L., Li, J.C., Singh, V.P. (2004), Two-dimensional kinematic wave model of overland-flow, *Journal of Hydrology*, 291, pp.28-41.

Liu, Q.Q., Chen, L., Li, J.C., Singh, V.P. (2005), Roll waves in overland flow, *Journal of Hydrologic Engineering*, 10(2), pp.110-117.

Ogden, F.L. and Julien, P.Y. (1993), Runoff sensitivity to temporal and spatial rainfall variability at runoff plane and small basin scales, *Water Resources Research*, 29(8), pp.2589-2597.

Saghafian, B. (2006), Nonlinear transformation of unit hydrograph, *Journal of Hydrology*, 330, pp.596-603.

Woolhiser, D.A., Smith, R.E., Giradez, J.V. (1996), Effects of spatial variability of saturated hydraulic conductivity on Hortonian overland flow, *Water Resources Research*, 32(3), pp.671-678.

Zanuttigh, B. and Lamberti, A. (2002), Roll waves simulation using shallow water equation and Weighted Average Flux method, *Journal of Hydraulic Research*, 40(5), pp.610-622.